THE JOURNAL OF PHYSICAL CHEMISTRY A

pubs.acs.org/JPCA Article

Mapping the Electronic Structure of the Uranium(VI) Dinitride Molecule, UN_2

Gaoxiang Liu, Chaoqun Zhang, Sandra M. Ciborowski, Ayush Asthana, Lan Cheng,* and Kit H. Bowen*

Cite This: J. Phys. Chem. A 2020, 124, 6486–6492 Read Online

ACCESS | Metrics & More | Article Recommendations | Supporting Information

ABSTRACT: A combined anion photoelectron spectroscopic and relativistic coupled-cluster computational study of the electronic structure of the UN_2 molecule is presented. Because the photoelectron spectrum of the uranium dinitride negative ion, UN_2^-, directly reflects the electronic structure of neutral UN_2, we have measured and relied upon the photoelectron spectrum of the UN_2^- anion as a means of mapping the electronic structure of neutral UN_2. In addition to the electron affinity of the UN_2 ground state, energy levels of the UN_2 excited states were well characterized by the close interplay between the experiment and high-level theory. We found that both electron attachment and electronic excitation significantly bend the UN_2 molecule and elongate its U≡N bond. Implications for the activation of UN_2 are discussed.

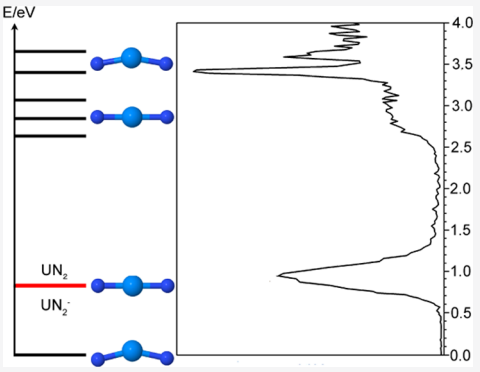

Downloaded via JOHNS HOPKINS UNIV on January 19, 2021 at 21:05:00 (UTC).
See https://pubs.acs.org/sharingguidelines for options on how to legitimately share published articles.

INTRODUCTION

Uranium nitrides are promising candidates as the fuel for generation IV power reactors. Currently, most nuclear fuel is in the form of uranium dioxide, UO_2. While uranium dioxide and uranium nitrides are all refractory materials, the attributes of uranium nitrides over uranium dioxide are their higher melting point, thermal conductivity, and fissionable density.[1,2] The bonding of nitrides, N^{3-}, with uranium has also stirred considerable interest in multiple bonding when an 5f orbital is involved. Plentiful research on uranium nitrides has focused on molecular uranium(VI) nitride complexes, which feature a [NUN] or a [U≡N] core with U in its highest oxidation state.[3−16] Despite these progresses, however, knowledge of uranium(VI) nitride chemistry has lagged behind that of the ubiquitous uranyl ion, UO_2^{2+}, whose U is also in the +6 oxidation state. The chemical bonding and electronic structure of uranyl complexes are well documented,[17] and it has made possible the manipulation of their coordination number, reactivity, and other properties.[18−21] Uranium(VI) nitride complexes, on the other hand, are relatively difficult to synthesize. Therefore, significant challenges are posed in regard to their characterization and the modification of their chemical and material properties.[3,4]

The behavior of uranium(VI) nitride complexes is, however, largely governed by the bonding between individual nitrogen and uranium, as well as the electronic properties of the uranium nitride unit. Therefore, isolated uranium nitride molecules are well suited for investigating the [NUN] core in uranium(VI) nitride complexes.[5] Previous work has explored individual uranium(VI) nitride molecules both in the gas phase and under matrix isolation conditions.[22−30] Infrared, microwave, and ionization spectroscopy have primarily characterized the ground-state properties of uranium(VI) nitride molecules. Experimental results on their electronic structure and excited-state properties, however, have been scarce. The dearth of experimental data necessitates guidance from theoretical calculations to predict and interpret their electronic structures. Nevertheless, accurate quantum-chemical calculations of excited states for uranium(VI) nitrides are challenging. The complexity of the electronic structure of the uranium atom demands that the theoretical method accounts for both electron correlation and relativistic effects accurately. Even for the isolated uranium dinitride molecule, UN_2, large discrepancies in computed excitation energies persist among different theoretical approaches.[31−38] For these reasons, the direct experimental measurement of the electronic structure for molecular uranium dinitrides is necessary. Such data, in partnership with accurate quantum-chemical calculations, have the potential of elucidating chemical bonding and electronic properties in uranium dinitride molecules and thus of providing a solid foundation for better understanding their behavior in bulkier uranium(VI) nitride complexes.

The photoelectron spectrum of the uranium dinitride negative ion, UN_2^-, directly reflects the electronic structure of neutral UN_2. For this reason, we have measured and relied

Received: April 27, 2020
Revised: July 23, 2020
Published: July 23, 2020

ACS Publications © 2020 American Chemical Society

https://dx.doi.org/10.1021/acs.jpca.0c03735
J. Phys. Chem. A 2020, 124, 6486–6492

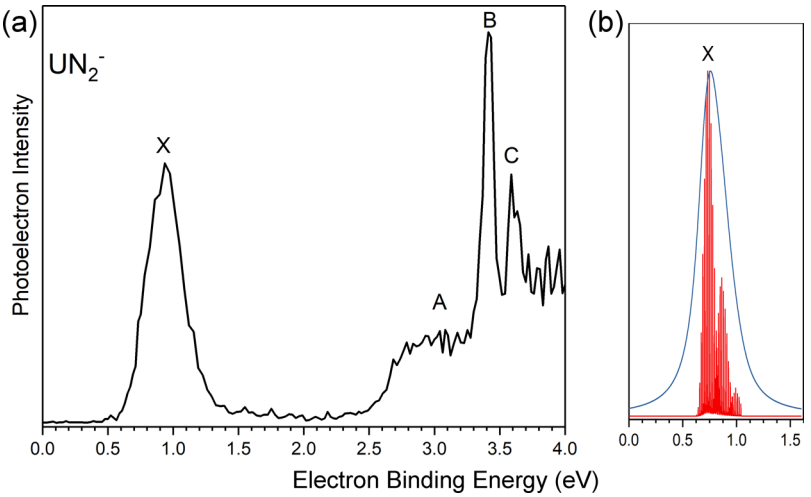

Figure 1. (a) Anion photoelectron spectrum of UN_2^-. (b) Simulated Franck−Condon spectrum for the transitions from the electronic ground state of the UN_2^- anion to that of neutral UN_2. The red lines were obtained by broadening the spectrum using Lorentzian functions with a full width at half-maximum (fwhm) of 0.01 eV for each vibrational transition, while the blue profile used a fwhm value of 0.15 eV, which corresponds the estimate of the present experimental resolution.

upon the photoelectron spectrum of the UN_2^- anion as a means of mapping the electronic structure of neutral UN_2. These anion photoelectron experiments, performed on gas-phase (isolated) uranium dinitride molecular anions, UN_2^-, have the additional advantage of being free of environmental perturbations. Both the ligands that interact with uranyl ions (UO_2^{2+}),[39−42] the isoelectronic cousins of UN_2 neutral molecules, and even the inert gases that envelop uranium nitrides in frozen matrices[43] are known to have pronounced effects on their host electronic structure. On the computational side of the theory−experiment partnership, quantum-chemical calculations using coupled-cluster methods[44,45] and relativistic exact two-component Hamiltonian[46−48] have been performed to facilitate the interpretation of the experimental photoelectron spectrum of UN_2^-. The computational methods used here[49,50] have recently been reported to provide systematically converged results for excitation energies of the uranyl ion.[51] They thus appear to be promising candidates for obtaining accurate results for excited states of UN_2. Here, we report a joint negative-ion photoelectron spectroscopic and relativistic coupled-cluster computational study of the electronic structure of uranium dinitride, that is, the neutral molecule, UN_2, in order to determine its ground- and excited-state energies and geometries. Evidence suggests that both electron attachment and electronic excitation readily break the linearity of UN_2, shedding light on the potential consequences of modifying the properties and reactivity of uranium nitride by electro- and/or photochemical means.

METHODS

Experimental Section. Anion photoelectron spectroscopy is conducted by crossing a mass-selected negative-ion beam with a fixed-energy photon beam and analyzing the energies of the resultant photodetached electrons. This technique is governed by the well-known energy-conserving relationship, $h\nu$ = EBE + EKE, where $h\nu$, EBE, and EKE are the photon energy, electron binding energy (photodetachment transition energy), and the electron kinetic energy, respectively. The details of our apparatus have been described elsewhere.[52] Briefly, the photoelectron spectra were collected on an apparatus consisting of an anion source, a linear time-of-flight mass spectrometer for mass analysis and selection, and a magnetic-bottle photoelectron spectrometer for electron energy analysis (resolution ∼35 meV at 1 eV EKE). The fourth harmonic (266 nm, 4.66 eV/photon) of Nd:YAG was used to photodetach electrons from the cluster anion of interest. Photoelectron spectra were calibrated against the well-known atomic lines of the copper anion, Cu^-. The UN_2^- anion was generated in a laser vaporization/reaction ion source.[53,54] It consisted of a depleted uranium (U-238) rod, which was ablated with second harmonic (60 mJ, 532 nm) photon pulses from a Nd:YAG laser and expanded with 100 psi of an ultrahigh purity helium−10% nitrogen gas mixture. The UN_2^- anion was also generated by expanding a helium−10% ammonia gas mixture over the uranium rod, as it was being laser ablated.

Computational. Coupled-cluster singles and doubles with noniterative inclusion of triple excitation [CCSD(T)][55] calculations with scalar-relativistic effects taken into account using the spin-free exact two-component theory in its one-electron variant (SFX2C-1e)[56,57] were carried out for the electronic ground states of UN_2^- and UN_2 to obtain equilibrium geometries and energies. Harmonic frequencies were obtained by means of numerical differentiation of analytic gradients. The local potential energy surfaces were scanned and fitted into a polynomial expansion containing up to sixth-order force constants. The details about the potential energy surfaces are documented in the Supporting Information. Using the fitted local potential energy surfaces, discrete variable representation (DVR)[58] calculations were performed to obtain the vibrational progression for the electronic ground state of UN_2 in the photodetachment spectrum of the anion, UN_2^-.

SFX2C-1e equation-of-motion excitation energy CCSD (EOMEE-CCSD)[59] calculations were carried out to obtain geometries for electronic excited states of UN_2. This provided a qualitative understanding of the features associated with the excited states of UN_2 in the photoelectron spectrum. To obtain a balanced description of the anion for comparison, SFX2C-1e EOM electron affinity CCSD (EOMEA-CCSD)[60] calculation was also performed for the equilibrium structure of the anion. EOM-CCSD calculations with spin−orbit coupling included at

https://dx.doi.org/10.1021/acs.jpca.0c03735
J. Phys. Chem. A 2020, 124, 6486−6492

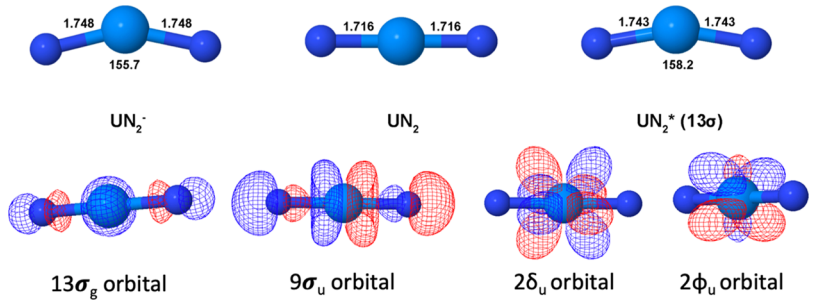

Figure 2. Computationally optimized structures of the electronic ground states of UN_2^- and UN_2 as well as of an electronically excited state of UN_2 with an excitation from the $9\sigma_u$ orbital into the $13\sigma_g$ orbital, labeled here as $UN_2^*(13\sigma)$. The $13\sigma_g$, $9\sigma_u$, $2\delta_u$, and $2\varphi_u$ orbitals are also presented.

Table 1. Experimental and X2CAMF-EOM-CCSD(T)(a)* Transition Energies for the Photodetachment Transitions from UN_2^- to the Ground and Excited States of UN_2[a]

		transition energy		R(U−N)	∠(N−U−N)
	electronic configuration	expt.	theo.	(in Å)	(in deg)
UN_2^-	$...9\sigma_u^2 7\pi_u^4 12\sigma_g^2 13\sigma_g^1$			1.748	155.7
	$...9\sigma_u^2 7\pi_u^4 12\sigma_g^2$ (S = 1)	0.6/0.93[b]	0.64/0.81[b]	1.716	180.0
UN_2	$...9\sigma_u^1 7\pi_u^4 12\sigma_g^2 2\varphi_u^1$ (S = 3)	2.6−3.3	2.41/2.54/3.10	1.768	180.0
	$...9\sigma_u^1 7\pi_u^4 12\sigma_g^2 2\delta_u^1$ (S = 3)		2.62/2.84/3.15	1.757	180.0
	$...9\sigma_u^1 7\pi_u^4 12\sigma_g^2 2\varphi_u^1$ (S = 1)		3.40	1.774	180.0
	$...9\sigma_u^1 7\pi_u^4 12\sigma_g^2 13\sigma_g^1$ (S = 3)	3.41	3.32/3.33/3.36	1.743[c]	158.2
	$...9\sigma_u^1 7\pi_u^4 12\sigma_g^2 13\sigma_g^1$ (S = 1)	3.59	3.65	1.742	155.9

[a]The geometries for the ground states of UN_2^- and UN_2 as well as for the excited states of UN_2 were obtained from SFX2C-1e-EOMEA-CCSD, CCSD(T), and EOM-CCSD calculations, respectively. [b]EA and VDEs, respectively. [c]This structure is a saddle point with respect to asymmetric stretching.

the orbital level using an X2C atomic mean-field approach (X2CAMF)[49,50] were performed to obtain accurate excitation energies for UN_2 at the SFX2C-1e-CCSD(T) geometry of the anion, which were added to the vertical detachment energy (VDE) calculated for the ground state to obtain VDEs for these excited states. Noniterative triple corrections were obtained using the CCSD(T)(a)* scheme[61] but with the correction to the similarity-transformed Hamiltonian accounted for using an expectation-value formulation in the same spirit as the CCSDR(3) method.[62] All SFX2C-1e calculations used the cc-pwCVTZ basis set for uranium[63] and the cc-pVTZ basis set for nitrogen[64] with SFX2C-1e contractions. The X2CAMF calculations used these basis sets in the uncontracted form, with virtual spinors higher than 100 hartree frozen in CC treatments. In all CC calculations presented here, uranium 1s, 2s, 2p, 3s, 3p, 3d, 4s, 4p, 4d, 4f, 5s, 5p, and 5d electrons and nitrogen 1s electrons were kept frozen. All calculations were carried out using the CFOUR[65−69] program package.

RESULTS AND DISCUSSION

Figure 1a presents the photoelectron spectrum of UN_2^- taken with a 266 nm (4.66 eV) laser. The spectrum exhibits multiple transitions with different shapes and intensities. Feature X reflects the transition from the ground electronic state of the UN_2^- anion to that of neutral UN_2. The threshold of this feature occurs at an EBE of 0.6 eV; it then reaches its intensity maximum at 0.93 eV. When there is a sufficient Franck−Condon overlap between the ground states of the anion and the neutral, the threshold of the first EBE feature, that is, 0.6 eV, corresponds to electron affinity (EA). Thus, the EA of the UN_2 molecule is 0.6 ± 0.05 eV. We interpret the weak intensity peaks between ∼0.4 and 0.5 eV to be vibrational hot bands. The first experimental VDE is the photodetachment transition at which the Franck−Condon overlap between the vibrational wave function of the electronic ground state of the anion and that of its neutral counterpart is maximal. Thus, the VDE value corresponds to the peak position of the first EBE feature. While this value was fitted to be 0.93 eV, the asymmetry on the low EBE side of the peak top suggests that the actual VDE value is less than 0.93 eV, perhaps by ∼0.1 eV. Furthermore, the width of feature X suggests an appreciable geometrical difference between the ground electronic states of the UN_2^- anion and neutral UN_2.

Because gas-phase data are not perturbed by environmental effects, they are ideally suited for direct comparisons with high-level quantum-chemical calculations. The properties for electronic ground states were modeled with SFX2C-1e-CCSD(T) calculations. As shown in Figure 2, the excess electron in the anion occupies the 13σ orbital and is mainly located in the U 7s orbital with a fraction in the O 2s and $2p_z$ orbitals. The equilibrium ground-state structure of the UN_2^- anion is bent with a N−U−N angle of 155.7°, while neutral UN_2 is linear at its electronic ground state (see Figure 2). In addition, the U−N bond length in UN_2^- (1.748 Å) is longer than that of UN_2 (1.716 Å). The computed EA and VDE are 0.64 and 0.81 eV, respectively; these values are in good agreement with the experimental results. Because of the large differences between the ground states of UN_2^- and UN_2 in terms of their bond angles and bond lengths, both bending and stretching modes are strongly active in photodetachment transition. The Franck−Condon simulation presented in Figure 1b reproduces the shape of feature X and implies that the long vibrational progression tail is primarily due to the symmetric stretch with progressions of the bending mode contributing to the finer structures. The corresponding

https://dx.doi.org/10.1021/acs.jpca.0c03735
J. Phys. Chem. A 2020, 124, 6486−6492

vibrational frequencies and Franck−Condon factors are given in Table S7 of the Supporting Information. The valence electronic configurations are summarized in Table 1. As orbitals of the anion in a bent structure (as well as those in excited states of the neutral molecule with bent geometries) largely retain the characteristics of those in the linear ground state of the neutral molecule, symbols for a linear molecule were used throughout to denote the molecular orbitals to facilitate intuitive understanding.

The structural distortion that an excess electron induces in UN_2 is analogous to that seen in the activation of CO_2. For both UN_2 and CO_2, an addition of an excess electron contributes repulsion with electrons in the π bonding orbitals and causes the bonds to bend and elongate. In the case of CO_2, these structural changes activate this otherwise stable, linear molecule and prepare it to undergo chemical reaction.[70−74] We thus anticipate that an excess electron also activates UN_2, endowing it with reactivity that enables its functionalization.

The good agreement seen here between the experiment and theory for the ground electronic states of UN_2^- and UN_2 establishes the foundation for the further study of excited-state properties. In the photoelectron spectrum of UN_2^-, features with electron binding energies higher than feature X correspond to photodetachment transitions from the ground electronic state of UN_2^- to the excited electronic states of neutral UN_2. Band A, which ranges from EBE ∼2.6 to 3.3 eV, is broad and weak, suggesting that it contains multiple transitions, some of which may be due to multielectron processes with low transition efficiencies. Electronic structure calculations show that band A is due to a collection of transitions from $9\sigma_u$ to $2\varphi_u$ or $2\delta_u$ orbitals (see Table 1), whose calculated transition energies range from 2.41 to 3.40 eV. $2\varphi_u$ or $2\delta_u$ orbitals essentially correspond to the U $5f_{\pm2}$ and $5f_{\pm1}$ orbitals (see Figure 2). Spin−orbit contributions significantly reduce these excitation energies, for example, by as large as 0.5 eV in the case of the triplet component of the $9\sigma_u \rightarrow 2\varphi_u$ transition (see the difference between SFX2C-1e-CCSD and X2CAMF-EOM-CCSD results in Table S1). We emphasize that spin−orbit coupling fundamentally changes these excitation energies of UN_2 instead of them just showing up as energy-level splittings. Triple corrections have a relatively small influence on these states and are consistently below 0.1 eV (see the difference between X2CAMF-EOM-CCSD and CCSD(T)(a)* results in Table S1). Because UN_2^- has an electron in its $13\sigma_g$ orbital, it can only transit to these neutral, electronically excited states via multielectron processes, further accounting for the low intensity of band A in the photoelectron spectrum.

Beyond band A are two sharp peaks located at EBE = 3.41 and 3.59 eV, labeled peak B and C, respectively. Their high intensities suggest strong, one-electron photodetachment transitions. Accurate X2CAMF-EOM-CCSD(T)(a)* calculations assign them respectively as the photodetachment transitions to the triplet and singlet $...9\sigma_u^1 7\pi_u^4 12\sigma_g^2 13\sigma_g^1$ states (hereafter abbreviated as the $13\sigma_g$ states) of UN_2. The calculated vertical transition energies, 3.32−3.36 and 3.65 eV, are in excellent agreement with the experimental EBE values. For these transitions, the spin−orbit coupling and triple contributions respectively amount to ∼0.2 and ∼0.3 eV. These effects are therefore crucially important for accurate calculations of electronically excited-state energies. In anion photoelectron spectroscopy, a sharp electronic transition peak with little vibrational broadening signifies a high structural similarity between the original (anion) and the final (neutral) states. The fact that peaks B and C are both sharp thus suggests that the 13σ excited states of UN_2 have geometries that are comparable to that of the UN_2^- anion; that is, they are all bent. This experimental observation is consistent with the geometry optimization, which reveals that UN_2 in its 13σ state has a similar structure to that of UN_2^- (see Table 1 and Figure 2). Therefore, in analogy to electron attachment to UN_2 activating it, that is, forming bent UN_2^-, the electronic excitation of UN_2 to particular excited states can also induce similar structural changes, that is, bending; these excited state-induced structural changes may also activate UN_2 and thus alter its reactivity.

While UN_2 in its triplet 13σ state is structurally similar to UN_2^-, this structure turns out to be unstable, that is, a saddle point, with respect to asymmetric stretching in scalar-relativistic EOM-CCSD calculations. Because we observe what appears to be that transition in the photoelectron spectrum, it may be that we are sampling the averaged C_{2v} structure in a relatively flat double-well potential. Spin−orbit coupling contributions may also be affecting the shape of the potential energy surface. A detailed characterization of potential energy surfaces of these excited states using the spin−orbit EOM-CC methods is beyond our current computational resources with analytical gradients for these new methods not being available yet.

The present calculations for excitation energies of UN_2 were carried out on the equilibrium structure of UN_2^-, while other reported high-level calculations[34−36] were performed on the equilibrium structure of the neutral molecule. Although this precludes a literal comparison, an inspection shows that the present X2CAMF-EOM-CCSD results are consistent with those obtained from spin−orbit effective-core-potential EOM-CCSD calculations.[35] A first study of the effects from triple excitations presented here serves to demonstrate the convergence and reliability of the EOM-CC results. Complete active space second-order perturbation theory calculations[36] seem to overestimate these excitation energies, perhaps indicating that it might improve results to enlarge the active space. Fock-space coupled cluster (FSCC) single and double calculations[34] seems to underestimate these excitation energies substantially. A similar observation has been reported in recent calculations for excitation energies of uranyl ions (UO_2^{2+}).[51] It thus seems of interest to further investigate the convergence of FSCC results with respect to the choices of the active space.

SUMMARY

In this paper, we present a combined anion photoelectron spectroscopic and relativistic coupled-cluster study of the electronic structure of the UN_2 molecule. UN_2 is much less characterized than its isoelectronic counterpart UO_2^{2+}. Energy levels of the UN_2 excited states are well characterized via the close interplay between the experiment and theory. We find that both electron attachment and electronic excitation significantly bend the UN_2 molecule and elongate its U≡N bond. This suggests that the morphology, coordination, and reactivity of UN_2 and the related uranium nitride compounds may be tuned using optical or electrochemical approaches. Knowledge of the electronic structure of uranium nitride may also be valuable in better understanding the behavior of uranium nitrides in nuclear reactors, where excited-state uranium nitrides may be prevalent.

https://dx.doi.org/10.1021/acs.jpca.0c03735
J. Phys. Chem. A 2020, 124, 6486−6492

■ ASSOCIATED CONTENT

Supporting Information

The Supporting Information is available free of charge at https://pubs.acs.org/doi/10.1021/acs.jpca.0c03735.

Detailed account of computed excitation energies using scalar relativistic method; three-dimensional discrete variable representation (DVR) calculations; equilibrium geometry parameters; fitting parameter; zero-point-energies; vibrational level; spin−orbit coupled-cluster methods with triples corrections; and details about the potential energy surfaces used in the DVR calculations (PDF)

■ AUTHOR INFORMATION

Corresponding Authors

Lan Cheng − *Department of Chemistry, Johns Hopkins University, Baltimore, Maryland 21218, United States;* orcid.org/0000-0003-1165-9559; Email: lcheng24@jhu.edu

Kit H. Bowen − *Department of Chemistry, Johns Hopkins University, Baltimore, Maryland 21218, United States;* orcid.org/0000-0002-2858-6352; Email: kbowen@jhu.edu

Authors

Gaoxiang Liu − *Department of Chemistry, Johns Hopkins University, Baltimore, Maryland 21218, United States;* orcid.org/0000-0002-1001-0064

Chaoqun Zhang − *Department of Chemistry, Johns Hopkins University, Baltimore, Maryland 21218, United States*

Sandra M. Ciborowski − *Department of Chemistry, Johns Hopkins University, Baltimore, Maryland 21218, United States;* orcid.org/0000-0001-9453-4764

Ayush Asthana − *Department of Chemistry, Johns Hopkins University, Baltimore, Maryland 21218, United States*

Complete contact information is available at: https://pubs.acs.org/10.1021/acs.jpca.0c03735

Notes

The authors declare no competing financial interest.

■ ACKNOWLEDGMENTS

The experimental material presented in this work was supported by The Department of Energy's Heavy Elements Chemistry Program (DOE-HEC) under grant number, DE-SC0019317 (K.H.B.). The computational material presented in this work was supported by The Department of Energy, Office of Science, Office of Basic Energy Sciences, under grant number DE-SC0020317 (L.C.). All computations in this work were carried out in the Maryland Advanced Research Computing Center (MARCC).

■ REFERENCES

(1) Matthews, R. B.; Chidester, K. M.; Hoth, C. W.; Mason, R. E.; Petty, R. L. Fabrication and Testing of Uranium Nitride Fuel for Space Power Reactors. *J. Nucl. Mater.* **1988**, *151*, 334−344.

(2) Streit, M.; Ingold, F. Nitrides as a Nuclear Fuel Option. *J. Eur. Ceram. Soc.* **2005**, *25*, 2687−2692.

(3) Thomson, R. K.; Cantat, T.; Scott, B. L.; Morris, D. E.; Batista, E. R.; Kiplinger, J. L. Uranium Azide Photolysis Results in C-H Bond Activation and Provides Evidence for a Terminal Uranium Nitride. *Nat. Chem.* **2010**, *2*, 723−729.

(4) Evans, W. J.; Kozimor, S. A.; Ziller, J. W. Molecular Octa-Uranium Rings with Alternating Nitride and Azide Bridges. *Science* **2005**, *309*, 1835−1838.

(5) King, D. M.; Liddle, S. T. Progress in Molecular Uranium-Nitride Chemistry. *Coord. Chem. Rev.* **2014**, *266−267*, 2−15.

(6) Fox, A. R.; Bart, S. C.; Meyer, K.; Cummins, C. C. Towards Uranium Catalysts. *Nature* **2008**, *455*, 341−349.

(7) Liddle, S. The Renaissance of Non-Aqueous Uranium Chemistry. *Angew. Chem., Int. Ed.* **2015**, *54*, 8604−8641.

(8) Diaconescu, P. Actinide Chemistry: A Tale of Two Nitrides. *Nat. Chem.* **2010**, *2*, 705−706.

(9) Cleaves, P. A.; Kefalidis, C. E.; Gardner, B. M.; Tuna, F.; McInnes, E. J. L.; Lewis, W.; Maron, L.; Liddle, S. T. Terminal Uranium(V/VI) Nitride Activation of Carbon Dioxide and Carbon Disulfide: Factors Governing Diverse and Well-Defined Cleavage and Redox Reactions. *Chem.—Eur. J.* **2017**, *23*, 2950−2959.

(10) Hayton, T. W. Recent Developments in Actinide−Ligand Multiple Bonding. *Chem. Commun.* **2013**, *49*, 2956−2973.

(11) Fox, A. R.; Cummins, C. C. Uranium−Nitrogen Multiple Bonding: The Case of a Four-Coordinate Uranium(VI) Nitridoborate Complex. *J. Am. Chem. Soc.* **2009**, *131*, 5716−5717.

(12) King, D. M.; Tuna, F.; McInnes, E. J. L.; McMaster, J.; Lewis, W.; Blake, A. J.; Liddle, S. T. Synthesis and Structure of a Terminal Uranium Nitride Complex. *Science* **2012**, *337*, 717−720.

(13) Evans, W. J. Molecular Octa-Uranium Rings with Alternating Nitride and Azide Bridges. *Science* **2005**, *309*, 1835−1838.

(14) King, D. M.; Tuna, F.; McInnes, E. J. L.; McMaster, J.; Lewis, W.; Blake, A. J.; Liddle, S. T. Isolation and Characterization of a Uranium (VI)−Nitride Triple Bond. *Nat. Chem.* **2013**, *5*, 482−488.

(15) Hayton, T. W. Synthesis of Imido Analogs of the Uranyl Ion. *Science* **2005**, *310*, 1941−1943.

(16) Fortier, S.; Wu, G.; Hayton, T. W. Synthesis of a Nitrido-Substituted Analogue of the Uranyl Ion, [N=U=O]+. *J. Am. Chem. Soc.* **2010**, *132*, 6888−6889.

(17) Denning, R. G. Electronic Structure and Bonding in Actinyl Ions and their Analogs. *J. Phys. Chem. A* **2007**, *111*, 4125−4143.

(18) Anderson, N. H.; Xie, J.; Ray, D.; Zeller, M.; Gagliardi, L.; Bart, S. C. Elucidating Bonding Preferences in Tetrakis(Imido)Uranate(VI) Dianions. *Nat. Chem.* **2017**, *9*, 850−855.

(19) Hayton, T. W. Understanding the Origins of O_{yl}−U−O_{yl} Bending in the Uranyl (UO_2^{2+}) Ion. *Dalton Trans.* **2018**, *47*, 1003−1009.

(20) Pedrick, E. A.; Schultz, J. W.; Wu, G.; Mirica, L. M.; Hayton, T. W. Perturbation of the O-U-O Angle in Uranyl by Coordination to a 12-Membered Macrocycle. *Inorg. Chem.* **2016**, *55*, 5693−5701.

(21) Szigethy, G.; Raymond, K. N. Hexadentate Terephthalamide-(bis-hydroxypyridinone) Ligands for Uranyl Chelation: Structural and Thermodynamic Consequences of Ligand Variation. *J. Am. Chem. Soc.* **2011**, *133*, 7942−7956.

(22) Green, D. W.; Reedy, G. T. The Identification of UN in Ar Matrices. *J. Chem. Phys.* **1976**, *65*, 2921−2922.

(23) Hunt, R. D.; Yustein, J. T.; Andrews, L. Matrix Infrared Spectra of NUN Formed by the Insertion of Uranium Atoms into Molecular Nitrogen. *J. Chem. Phys.* **1993**, *98*, 6070−6074.

(24) Kushto, G. P.; Souter, P. F.; Andrews, L.; Neurock, M. A Matrix Isolation FT−IR and Quasirelativistic Density Functional Theory Investigation of the Reaction Products of Laser-Ablated Uranium Atoms with NO, NO_2 and N_2O. *J. Chem. Phys.* **1997**, *106*, 5894−5903.

(25) Kushto, G. P.; Souter, P. F.; Andrews, L. An Infrared Spectroscopic and Quasirelativistic Theoretical Study of the Coordination and Activation of Dinitrogen by Thorium and Uranium Atoms. *J. Chem. Phys.* **1998**, *108*, 7121−7130.

(26) Andrews, L.; Wang, X.; Lindh, R.; Roos, B. O.; Marsden, C. J. Simple N≡UF_3 and P≡UF_3 Molecules with Triple Bonds to Uranium. *Angew. Chem., Int. Ed.* **2008**, *47*, 5366−5370.

(27) Andrews, L.; Wang, X.; Gong, Y.; Vlaisavljevich, B.; Gagliardi, L. Infrared Spectra and Electronic Structure Calculations for the

$NUN(NN)_{1-5}$ and $NU(NN)_{1-6}$ Complexes in Solid Argon. *Inorg. Chem.* **2013**, *52*, 9989−9993.
(28) Vlaisavljevich, B.; Andrews, L.; Wang, X.; Gong, Y.; Kushto, G. P.; Bursten, B. E. Detection and Electronic Structure of Naked Actinide Complexes: Rhombic-Ring $(AnN)_2$ Molecules Stabilized by Delocalized π-Bonding. *J. Am. Chem. Soc.* **2016**, *138*, 893−905.
(29) Matthew, D. J.; Morse, M. D. Resonant Two-Photon Ionization Spectroscopy of Jet-Cooled UN: Determination of the Ground State. *J. Chem. Phys.* **2013**, *138*, 184303.
(30) Battey, S. R.; Bross, D. H.; Peterson, K. A.; Persinger, T. D.; VanGundy, R. A.; Heaven, M. C. Spectroscopic and Theoretical Studies of UN and UN^+. *J. Chem. Phys.* **2020**, *152*, 094302.
(31) Gagliardi, L.; Roos, B. O. Uranium Triatomic Compounds XUY (X, Y=C, N, O): A Combined Multiconfigurational Second-Order Perturbation and Density Functional Study. *Chem. Phys. Lett.* **2000**, *331*, 229−234.
(32) Réal, F.; Vallet, V.; Marian, C.; Wahlgren, U. Theoretical Investigation of the Energies and Geometries of Photoexcited Uranyl(VI) Ion: A Comparison Between Wave-Function Theory and Density Functional Theory. *J. Chem. Phys.* **2007**, *127*, 214302.
(33) Kaltsoyannis, N. Computational Study of Analogues of the Uranyl Ion Containing the -N=U=N- Unit: Density Functional Theory Calculations on UO_2^{2+}, UON^+, UN_2, $UO(NPH_3)^{3+}$, $U(NPH_3)_2^{4+}$, $[UCl_4\{NPR_3\}_2]$ (R = H, Me), and $[UOCl_4\{NP(C_6H_5)_3\}]^-$. *Inorg. Chem.* **2000**, *39*, 6009−6017.
(34) Tecmer, P.; Gomes, A. S. P.; Knecht, S.; Visscher, L. Communication: Relativistic Fock-Space Coupled Cluster Study of Small Building Blocks of Larger Uranium Complexes. *J. Chem. Phys.* **2014**, *141*, 041107.
(35) Zhang, S.; Wang, F. Excitation Energies of UO_2^{2+}, NUO^+, and NUN Based on Equation-of- Motion Coupled-Cluster Theory with Spin−Orbit Coupling. *J. Phys. Chem. A* **2017**, *121*, 3966−3975.
(36) Wei, F.; Wu, G.; Schwarz, W. H. E.; Li, J. Geometries, Electronic Structures, and Excited States of UN_2, NUO^+, and UO_2^{2+}: A Combined CCSD(T), RAS/CASPT2 and TDDFT Study. *Theor. Chem. Acc.* **2011**, *129*, 467−481.
(37) Tecmer, P.; Gomes, A. S. P.; Ekström, U.; Visscher, L. Electronic Spectroscopy of UO_2^{2+}, NUO^+ and NUN: An Evaluation of Time-Dependent Density Functional Theory for Actinides. *Phys. Chem. Chem. Phys.* **2011**, *13*, 6249−6259.
(38) Todorova, T. K.; Gagliardi, L.; Walensky, J. R.; Miller, K. A.; Evans, W. J. DFT and CASPT2 Analysis of Polymetallic Uranium Nitride and Oxide Complexes: How Theory Can Help When X-Ray Analysis Is Inadequate. *J. Am. Chem. Soc.* **2010**, *132*, 12397−12403.
(39) Su, J.; Li, W.-L.; Lopez, G. V.; Jian, T.; Cao, G.-J.; Li, W.-L.; Schwarz, W. H. E.; Wang, L.-S.; Li, J. Probing the Electronic Structure and Chemical Bonding of MonoUranium Oxides with Different Oxidation States: UO_x^- and UO_x (x = 3−5). *J. Phys. Chem. A* **2016**, *120*, 1084−1096.
(40) Su, J.; Dau, P. D.; Qiu, Y.-H.; Liu, H.-T.; Xu, C.-F.; Huang, D.-L.; Wang, L.-S.; Li, J. Probing the Electronic Structure and Chemical Bonding in Tricoordinate Uranyl Complexes $UO_2X_3^-$ (X = F, Cl, Br, I): Competition between Coulomb Repulsion and U−X Bonding. *Inorg. Chem.* **2013**, *52*, 6617−6626.
(41) Dau, P. D.; Su, J.; Liu, H.-T.; Liu, J.-B.; Huang, D.-L.; Li, J.; Wang, L.-S. Observation and Investigation of the Uranyl Tetrafluoride Dianion $(UO_2F_4^{2-})$ and its Solvation Complexes with Water and Acetonitrile. *Chem. Sci.* **2012**, *3*, 1137−1146.
(42) Jin, J.; Gondalia, R.; Heaven, M. C. Electronic Spectroscopy of UO_2Cl_2 Isolated in Solid Ar. *J. Phys. Chem. A* **2009**, *113*, 12724−12728.
(43) Gagliardi, L.; Heaven, M. C.; Krogh, J. W.; Roos, B. O. The Electronic Spectrum of the UO_2 Molecule. *J. Am. Chem. Soc.* **2005**, *127*, 86−91.
(44) Bartlett, R. J.; Musiał, M. Coupled-Cluster Theory in Quantum Chemistry. *Rev. Mod. Phys.* **2007**, *79*, 291−352.
(45) Crawford, T. D.; Schaefer, H. F. An Introduction to Coupled Cluster Theory for Computational Chemists. *Rev. Comput. Chem.* **2007**, *14*, 33.
(46) Dyall, K. G. Interfacing Relativistic and Nonrelativistic Methods. I. Normalized Elimination of the Small Component in the Modified Dirac Equation. *J. Chem. Phys.* **1997**, *106*, 9618.
(47) Kutzelnigg, W.; Liu, W. Quasirelativistic Theory Equivalent to Fully Relativistic Theory. *J. Chem. Phys.* **2005**, *123*, 241102.
(48) Iliaš, M.; Saue, T. An Infinite-Order Two-Component Relativistic Hamiltonian by a Simple One-Step Transformation. *J. Chem. Phys.* **2007**, *126*, 064102.
(49) Liu, J.; Cheng, L. An Atomic Mean-Field Spin-Orbit Approach within Exact Two-Component Theory for a Non-perturbative Treatment of Spin-Orbit Coupling. *J. Chem. Phys.* **2018**, *148*, 144108.
(50) Asthana, A.; Liu, J.; Cheng, L. Exact Two-Component Equation-of-Motion Coupled-Cluster Singles and Doubles Method using Atomic Mean-Field Spin-Orbit Integrals. *J. Chem. Phys.* **2019**, *150*, 074102.
(51) Cheng, L. Study of Non-iterative Triples Contributions in Relativistic Equation-of-Motion Coupled-Cluster Calculations using an Exact Two-Component Hamiltonian with Atomic Mean-Field Spin-Orbit Integrals: Application to Uranyl and Other Heavy-Element Compounds. *J. Chem. Phys.* **2019**, *151*, 104103.
(52) Liu, G.; Pinkard, A.; Ciborowski, S. M.; Chauhan, V.; Zhu, Z.; Aydt, A. P.; Khanna, S. N.; Roy, X.; Bowen, K. H. Tuning the Electronic Properties of Hexanuclear Cobalt Sulfide Superatoms via Ligand Substitution. *Chem. Sci.* **2019**, *10*, 1760−1766.
(53) Liu, G.; Miliordos, E.; Ciborowski, S. M.; Tschurl, M.; Boesl, U.; Heiz, U.; Zhang, X.; Xantheas, S. S.; Bowen, K. Communication: Water Activation and Splitting by Single Metal-Atom Anions. *J. Chem. Phys.* **2018**, *149*, 221101.
(54) Liu, G.; Zhu, Z.; Ciborowski, S. M.; Ariyarathna, I. R.; Miliordos, E.; Bowen, K. H. Selective Activation of the C−H Bond in Methane by Single Platinum Atomic Anions. *Angew. Chem., Int. Ed.* **2019**, *131*, 7855−7859.
(55) Raghavachari, K.; Trucks, G. W.; Pople, J. A.; Head-Gordon, M. A Fifth-Order Perturbation Comparison of Electron Correlation Theories. *Chem. Phys. Lett.* **1989**, *157*, 479−483.
(56) Dyall, K. G. Interfacing relativistic and nonrelativistic methods. IV. One- and Two-Electron Scalar Approximations. *J. Chem. Phys.* **2001**, *115*, 9136.
(57) Liu, W.; Peng, D. Exact Two-Component Hamiltonians Revisited. *J. Chem. Phys.* **2009**, *131*, 031104.
(58) Colbert, D. T.; Miller, W. H. A Novel Discrete Variable Representation for Quantum Mechanical Reactive Scattering via the S-matrix Kohn Method. *J. Chem. Phys.* **1992**, *96*, 1982−1991.
(59) Stanton, J. F.; Bartlett, R. J. The Equation of Motion Coupled-Cluster Method. A Systematic Biorthogonal Approach to Molecular Excitation Energies, Transition Probabilities, and Excited State Properties. *J. Chem. Phys.* **1993**, *98*, 7029.
(60) Nooijen, M.; Bartlett, R. J. Equation of Motion Coupled Cluster Method for Electron Attachment. *J. Chem. Phys.* **1995**, *102*, 3629.
(61) Matthews, D. A.; Stanton, J. F. A New Approach to Approximate Equation-of-Motion Coupled Cluster with Triple Excitations. *J. Chem. Phys.* **2016**, *145*, 124102.
(62) Christiansen, O.; Koch, H.; Jo/rgensen, P. Perturbative Triple Excitation Corrections to Coupled Cluster Singles and Doubles Excitation Energies. *J. Chem. Phys.* **1996**, *105*, 1451.
(63) Peterson, K. A. Correlation Consistent Basis Sets for Actinides. I. The Th and U Atoms. *J. Chem. Phys.* **2015**, *142*, 074105.
(64) Dunning, T. H. Gaussian Basis Sets for Use in Correlated Molecular Calculations. I. The Atoms Boron through Neon and Hydrogen. *J. Chem. Phys.* **1989**, *90*, 1007−1023.
(65) Matthews, D. A.; Cheng, L.; Harding, M. E.; Lipparini, F.; Stopkowicz, S.; Jagau, T.-C.; Szalay, P. G.; Gauss, J.; Stanton, J. F. Coupled-Cluster Techniques for Computational Chemistry: The CFOUR Program Package. *J. Chem. Phys.* **2020**, *152*, 214108.
(66) CFOUR. *Coupled-Cluster Techniques for Computational Chemistry*, a quantum-chemical program package by Stanton, J. F.; Gauss, J.; Cheng, L.; Harding, M. E.; Matthews, D. A.; Szalay, P. G.; with contributions from Auer, A. A.; Bartlett, R. J.; Benedikt, U.;

https://dx.doi.org/10.1021/acs.jpca.0c03735
J. Phys. Chem. A 2020, 124, 6486−6492

Berger, C.; Bernholdt, D. E.; Bomble, Y. J.; Christiansen, O.; Engel, F.; Faber, R.; Heckert, M.; Heun, O.; Hilgenberg, M.; Huber, C.; Jagau, T.-C.; Jonsson, D.; Jusélius, J.; Kirsch, T.; Klein, K.; Lauderdale, W.J.; Lipparini, F.; Metzroth, T.; Mück, L.A.; O'Neill, D.P.; Price, D.R.; Prochnow, E.; Puzzarini, C.; Ruud, K.; Schiffmann, F.; Schwalbach, W.; Simmons, C.; Stopkowicz, S.; Tajti, A.; Vázquez, J.; Wang, F.; Watts, J. D.; and the integral packages MOLECULE (Almlöf, J.; Taylor, P. R.), PROPS (Taylor, P. R.), ABACUS (Helgaker, T.; Jensen, H. J. A.; Jørgensen, P.; Olsen, J.), and ECP routines by Mitin, A. V.; van Wüllen, C. For the current version, see http://www.cfour.de.

(67) Watts, J. D.; Gauss, J.; Bartlett, R. J. Coupled-cluster Methods with Noniterative Triple Excitations for Restricted Open-Shell Hartree−Fock and Other General Single Determinant Reference Functions. Energies and Analytical Gradients. *J. Chem. Phys.* **1993**, *98*, 8718.

(68) Stanton, J. F.; Gauss, J. Analytic Energy Gradients for the Equation-of-Motion Coupled-Cluster Method: Implementation and Application to the HCN/HNC System. *J. Chem. Phys.* **1994**, *100*, 4695.

(69) Cheng, L.; Gauss, J. Analytic Energy Gradients for the Spin-Free Exact Two-Component Theory using an Exact Block Diagonalization for the One-Electron Dirac Hamiltonian. *J. Chem. Phys.* **2011**, *135*, 084114.

(70) Lee, S. H.; Kim, N.; Ha, D. G.; Kim, S. K. "Associative" Electron Attachment to Azabenzene−$(CO_2)_n$ van der Waals Complexes: Stepwise Formation of Covalent Bonds with Additive Electron Affinities. *J. Am. Chem. Soc.* **2008**, *130*, 16241.

(71) Kamrath, M. Z.; Relph, R. A.; Johnson, M. A. Vibrational Predissociation Spectrum of the Carbamate Radical Anion, C_5H_5N-CO_2^-, Generated by Reaction of Pyridine with $(CO_2)_m^-$. *J. Am. Chem. Soc.* **2010**, *132*, 15508−15511.

(72) Dodson, L. G.; Thompson, M. C.; Weber, J. M. Characterization of Intermediate Oxidation States in CO_2 Activation. *Annu. Rev. Phys. Chem.* **2018**, *69*, 231−252.

(73) Liu, G.; Poths, P.; Zhang, X.; Zhu, Z.; Marshall, M.; Blankenhorn, M.; Alexandrova, A. N.; Bowen, K. H. CO_2 Hydrogenation to Formate and Formic Acid by Bimetallic Palladium−Copper Hydride Clusters. *J. Am. Chem. Soc.* **2020**, *142*, 7930−7936.

(74) Liu, G.; Ciborowski, S. M.; Zhu, Z.; Chen, Y.; Zhang, X.; Bowen, K. H. The Metallo-Formate Anions, $M(CO_2)^-$, M=Ni, Pd, Pt, Formed by Electron-Induced CO_2 Activation. *Phys. Chem. Chem. Phys.* **2019**, *21*, 10955−10960.

https://dx.doi.org/10.1021/acs.jpca.0c03735
J. Phys. Chem. A 2020, 124, 6486−6492